Spin-resolved electron waiting times in a quantum-dot spin valve

Gaomin Tang,[1] Fuming Xu,[2,*] Shuo Mi,[1,3] and Jian Wang[1,†]

[1]*Department of Physics and the Center of Theoretical and Computational Physics, The University of Hong Kong, Hong Kong, China*

[2]*Shenzhen Key Laboratory of Advanced Thin Films and Applications, College of Physics and Energy, Shenzhen University, Shenzhen 518060, China*

[3]*Department of Applied Physics, Aalto University, 00076 Aalto, Finland*

(Received 1 December 2017; revised manuscript received 9 February 2018; published 5 April 2018)

We study the electronic waiting-time distributions (WTDs) in a noninteracting quantum-dot spin valve by varying spin polarization and the noncollinear angle between the magnetizations of the leads using the scattering matrix approach. Since the quantum-dot spin valve involves two channels (spin up and down) in both the incoming and outgoing channels, we study three different kinds of WTDs, which are two-channel WTD, spin-resolved single-channel WTD, and cross-channel WTD. We analyze the behaviors of WTDs in short times, correlated with the current behaviors for different spin polarizations and noncollinear angles. Cross-channel WTD reflects the correlation between two spin channels and can be used to characterize the spin-transfer torque process. We study the influence of the earlier detection on the subsequent detection from the perspective of cross-channel WTD, and define the influence degree quantity as the cumulative absolute difference between cross-channel WTDs and first-passage time distributions to quantitatively characterize the spin-flip process. We observe that influence degree versus spin-transfer torque for different noncollinear angles as well as different polarizations collapse into a single curve showing universal behaviors. This demonstrates that cross-channel WTDs can be a pathway to characterize spin correlation in spintronics system.

DOI: 10.1103/PhysRevB.97.165407

I. INTRODUCTION

Spintronics, which utilizes the spin degree of freedom to process and store information in nanostructured devices, has received intensive research in the past decades [1–3]. In spintronics, the magnetic tunnel junction (MTJ) is of particular interest, which typically consists of two ferromagnetic leads separated by an insulating layer such as a Fe/MgO/Fe junction [4–6]. The spin-polarized current varies with the spin polarization and the relative directions of magnetization in the magnetic layers. In general, the tunneling current of parallel configuration of the two magnetic layers is much larger than that of antiparallel configuration, and this is the so-called tunnel magnetoresistance (TMR) [6–11]. As predicted independently by Slonczewski [12] and Berger [13] in 1996, spin current is not conserved through the MTJ with noncollinear magnetizations in the magnetic layers, which can induce a spin-transfer torque (STT) on the magnetization [14–18]. STT has been applied on spintronic devices such as STT magnetoresistive random-access memory (STT-MRAM), which employs the STT instead of the magnetic field to control the magnetization and hence has lower power consumption [19]. Other investigations of MTJ include the spin-dependent Seebeck effect in the thermoelectric engine [20–24], angle-dependent conductance [25–27], adiabatic pumping [28,29], etc. The quantum-dot (QD) spin valve is related to MTJ, and has both the TMR and STT effect as well. If one tunes the QD levels far away from the resonant condition, it can mimic the behaviors of MTJ with an insulating scattering region. Yu *et al.* has shown that the off-resonant behaviors of the spin torque of a QD spin valve are the same as that of MTJ [30].

Current and its fluctuation are typical characterizations of quantum transport properties in nanodevices [31]. A more general description beyond current and fluctuation should resort to the formalism of full-counting statistics (FCS), which can give a full scenery of probability distribution of transferred charges and all zero-frequency cumulants at long times [32–46]. The FCS of charge and STT in an MTJ and QD spin valve has received intensive attention [29,39,47], and magnetization switching probability can also be evaluated via FCS [48]. With the rapid development of single-electron devices [49–51], a deeper understanding of important information on short-time physics becomes possible. However, FCS usually deals with collective behaviors of many electrons at long times and the short-time particle dynamics is lost. As a complement to FCS, electronic waiting-time distribution (WTD) has been developed to characterize the short-time correlation in mesoscopic conductors, which is the probability density of delay times between two subsequent charge transfers [52]. WTDs have been studied for systems governed by either Markovian [53–60] or non-Markovian [61] master equations. The scattering matrix formalism [35] has been developed to calculate WTDs under both constant voltage [62,63] and periodic drive [64–66]. A quantum theory of waiting-time clock has been developed in order to measure WTDs experimentally [67]. Generalization to multiple channels [68,69] has been made and the formalism of joint WTD [69], which characterizes the correlation between subsequent times, has been established. Spin-averaged WTD in a QD spin valve has been studied by Sothmann [57].

*xufuming@szu.edu.cn

†jianwang@hku.hk

Since the spintronic phenomenon plays an indispensable role in fundamental research and industrial application, investigation of WTD in the spintronic system is very important. Study of the spin-resolved WTD of the spintronic system, which involves at least two channels (spin up and down), is still lacking and the lacuna should be filled. We note that QD spin valve or MTJ are earlier examples in the family of spintronics. In this work, we employ multichannel WTD formalism and study WTDs and cross-channel WTDs of the QD spin valve using a scattering matrix approach. The scattering matrix approach requires the electronic reservoir to have a linear dispersion with respect to the momentum in the transport window and the system at zero temperature. We employ the nonequilibrium Green's function technique, which does not rely on weak-coupling strength between QD and electrodes, to get the scattering amplitude. The behaviors of two channel, spin-σ and cross-channel, WTDs are numerically calculated with respect to noncollinear angle and spin polarization, and their behaviors at initial short times are identified and explained. The difference between cross-channel WTD and the corresponding first-passage time distribution (FPTD) reveals the influence of the first detection on the subsequent one, and indicates the correlation between spin channels. In order to characterize the correlation strength between spin channels quantitatively, we introduce the "influence degree" quantity as the cumulative absolute difference between cross-channel WTDs and FPTDs. We find that the influence degree vanishes for collinear configurations and reaches its maximum near noncollinear angle $\theta = \pi/2$ in which STT also achieves its maximal value. Since spin-correlation strength increases with increasing spin polarization, influence degree is an increasing function with respect to the spin polarization.

The paper is organized as follows. In Sec. II, the system setup and theoretical formalism of two-channel WTD are introduced. We also present the spin-resolved waiting-time clock in this section. In Sec. III, we show the numerical results of WTD by varying the spin polarization and the angle between the magnetizations of the leads in detail, accompanied by discussion and analysis. Finally, we summarize our work in Sec. IV.

II. MODEL AND THEORETICAL FORMALISM

A. Magnetic tunnel junction

The spin valve we consider consists of a QD coupled to its left and right ferromagnetic leads $\alpha = L,R$, with the magnetization of the left lead at a noncollinear angle of θ to the magnetization of the right lead (Fig. 1). We consider a large QD so that the Coulomb interaction effect can be neglected. The system Hamiltonian reads as

$$H = H_S + \sum_{\alpha=L,R} (H_\alpha + H_{\alpha S}). \tag{1}$$

Here, the Hamiltonian of the noninteracting QD is expressed as

$$H_S = \sum_\sigma \epsilon_\sigma d_\sigma^\dagger d_\sigma, \tag{2}$$

where $\epsilon_\uparrow$ and $\epsilon_\downarrow$ can be different for a quantum spin Hall (QSH) QD [70–72] due to the Zeeman splitting in the presence of a magnetic field. And H_α describes the Hamiltonians of the left and right leads in the local reference frame with the form

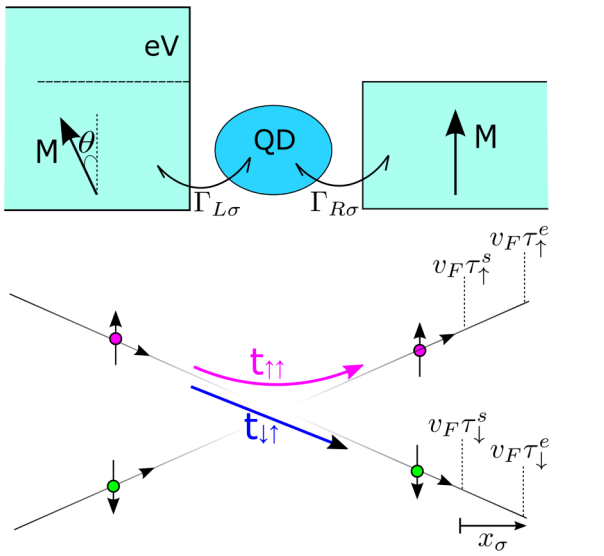

FIG. 1. Schematic illustration of a spin valve in which a QD coupled to its left and right ferromagnetic leads $\alpha = L,R$ through coupling strengths $\Gamma_{\alpha\sigma}$. The magnetization of the right lead is along the z axis, while that of the left lead is along the z' axis at a noncollinear angle of θ to the z axis. The transmitted electrons with spin σ are detected in the outgoing channels (right lead) at different positions, $x_\sigma \in [v_F\tau_\sigma^s, v_F\tau_\sigma^e]$.

$$H_\alpha = \sum_{k\sigma} \epsilon_{k\alpha\sigma} c_{k\alpha\sigma}^\dagger c_{k\alpha\sigma}, \tag{3}$$

where $\epsilon_{k\alpha\sigma}$ is the energy of an electron with spin σ and wave number k in the α ferromagnetic lead. The coupling Hamiltonians between the QD and the left and right leads are [27]

$$\begin{aligned} H_{LC} &= \sum_k c_{kL}^\dagger t_L \mathcal{R} d + \text{H.c.}, \\ H_{RC} &= \sum_k c_{kR}^\dagger t_R d + \text{H.c.}, \end{aligned} \tag{4}$$

respectively, where we used the abbreviations $c_{k\alpha}^\dagger = (c_{k\alpha\uparrow}^\dagger, c_{k\alpha\downarrow}^\dagger)$ and $d^\dagger = (d_\uparrow^\dagger, d_\downarrow^\dagger)$. Here, $t_\alpha = \text{diag}(t_{\alpha\uparrow}, t_{\alpha\downarrow})$ is the hopping matrix elements between the QD and the spin-σ electronic states in the lead α when $\theta = 0$. The rotation matrix $\mathcal{R}$ from the Bogoliubov transformation is applied to diagonalize the Hamiltonian of the left lead and has the form [39]

$$\mathcal{R} = \begin{pmatrix} \cos\frac{\theta}{2} & -\sin\frac{\theta}{2} \\ \sin\frac{\theta}{2} & \cos\frac{\theta}{2} \end{pmatrix}. \tag{5}$$

The coupling strength between the QD and leads in the collinear configuration is described by $\Gamma_{\alpha\sigma} = 2\pi |t_\alpha|^2 \rho_{\alpha\sigma}$, and we set $\Gamma_\alpha = (\Gamma_{\alpha\uparrow} + \Gamma_{\alpha\downarrow})/2$. $\rho_{\alpha\sigma}$ is the density of states for the spin σ electrons in the lead α. The spin polarization p_α in the lead α is given by

$$p_\alpha = \frac{\rho_{\alpha\uparrow} - \rho_{\alpha\downarrow}}{\rho_{\alpha\uparrow} + \rho_{\alpha\downarrow}} = \frac{\Gamma_{\alpha\uparrow} - \Gamma_{\alpha\downarrow}}{\Gamma_{\alpha\uparrow} + \Gamma_{\alpha\downarrow}}. \tag{6}$$

$p_\alpha = 0$ indicates that lead α is a normal metal and $p_\alpha = 1$ denotes a half-metallic ferromagnet. Then the coupling strength can be written as $\Gamma_{\alpha\sigma} = \Gamma_\alpha(1 + \sigma p_\alpha)/2$, with $\sigma = 1$ for spin up and $\sigma = -1$ for spin down. In this work, we assume the system is symmetric and both leads have the same coupling strength, $\Gamma_L = \Gamma_R \equiv \Gamma$, and the same polarization, $p_L = p_R \equiv p$.

The retarded Green's function of the central QD in spin space is

$$\mathbf{G}^r(E) = \left(E - H_0 - \mathcal{R}\Sigma_L^r\mathcal{R}^\dagger - \Sigma_R^r\right)^{-1}, \tag{7}$$

where $H_0 = \mathrm{diag}(\epsilon_\uparrow, \epsilon_\downarrow)$, and the retarded self-energy in the lead α is $\Sigma^r_{\alpha\sigma} = -i\Gamma_{\alpha\sigma}/2$. The transmission matrix from the left lead to the right lead is $\mathbf{T} = \mathbf{G}^r\mathcal{R}\Gamma_L\mathcal{R}^\dagger\mathbf{G}^a\Gamma_R$, with $\Gamma_\alpha = \mathrm{diag}(\Gamma_{\alpha\uparrow}, \Gamma_{\alpha\downarrow})$ and $\mathbf{G}^a = [\mathbf{G}^r]^\dagger$. The transmission amplitude matrix, which consists of the scattering matrix elements relating the left and right leads, can be obtained using the Fisher-Lee relation and expressed as [73–75]

$$\mathbf{t} = \begin{pmatrix} t_{\uparrow\uparrow} & t_{\uparrow\downarrow} \\ t_{\downarrow\uparrow} & t_{\downarrow\downarrow} \end{pmatrix} = \sqrt{\Gamma_R}\mathbf{G}^r\mathcal{R}\sqrt{\Gamma_L}, \tag{8}$$

with its component $t_{\sigma\sigma'}$ denoting the transmission amplitude from spin σ' in the left lead to spin σ in the right lead. The explicit energy E dependence of the transmission amplitude matrix is suppressed for notational simplicity. The QD spin valve is driven out of equilibrium by applying a constant voltage bias V. The transport window is $[E_F, E_F + eV]$, with E_F the Fermi level at zero temperature. The spin current in the left and right leads is, respectively, expressed as

$$I_{L\sigma} = \int_0^{eV} [\mathbf{t}^\dagger\mathbf{t}]_{\sigma\sigma} dE, \quad I_{R\sigma} = \int_0^{eV} [\mathbf{t}\mathbf{t}^\dagger]_{\sigma\sigma} dE. \tag{9}$$

The particle current through the system is expresses as

$$I = \int_0^{eV} \mathrm{Tr}[\mathbf{t}\mathbf{t}^\dagger] dE. \tag{10}$$

The spin-transfer torque is given by [30]

$$\mathbf{T}_s = \int_0^{eV} \mathrm{Tr}\left[\mathbf{G}^r\left(i\Sigma_L^a\bar{\mathcal{R}} - i\bar{\mathcal{R}}\Sigma_L^r\right)\mathbf{G}^a\Gamma_R\right] dE, \tag{11}$$

with

$$\bar{\mathcal{R}} = \begin{pmatrix} -\sin\theta & \cos\theta \\ \cos\theta & \sin\theta \end{pmatrix}. \tag{12}$$

B. Waiting-time distributions

In this section, we discuss the formalism to calculate waiting times between successive electrons detected in the right lead. The system has two incoming and two outgoing channels, namely, spin up and spin down. If one detects an electron at a starting time τ^s, the conditional probability density of detecting the successive electron at an ending time τ^e is the two-channel WTD $\mathcal{W}(\tau^s, \tau^e)$. The detection involved in the two-channel WTD does not differentiate the electron spin. One can also define the spin-resolved WTD $\mathcal{W}_{\sigma\sigma'}(\tau^s, \tau^e)$, which is the conditional probability density to detect a spin σ' electron at an ending time τ^e on the condition that the starting detection of the spin σ electron occurred at the earlier time τ^s. If the two successively detected electrons possess the same spin, it is the spin-resolved single-channel WTD, while if the two successive electrons have different spins, one can define it as the cross-channel WTD [69]. Since the dc case is considered here, WTD only depends on the time difference $\tau = \tau^e - \tau^s$ due to the time translational symmetry, and one can write the above-defined WTDs as $\mathcal{W}(\tau)$ and $\mathcal{W}_{\sigma\sigma'}(\tau)$, respectively. Before coming back to the discussion of WTDs, we first discuss the idle-time probability (ITP) which plays the role of the generating function of WTDs.

We use the scattering matrix approach, which was initially developed by Hassler *et al.* [35] and then generalized to the multichannel case by Dasenbrook *et al.* [69], to evaluate the ITPs in noninteracting systems at zero temperature. The scattering matrix approach requires a linear dispersion relation with respect to the momentum in the transport window $[E_F, E_F + eV]$,

$$E(k) = \hbar k v_F, \tag{13}$$

where the energy $E(k)$ is measured with respect to the Fermi level and v_F is the Fermi velocity. We assume that the Fermi velocities for spin-up and -down electrons are the same and no spin bias is present in this work. Instead of considering the probability of no spin-σ electrons detected in the time intervals $[\tau_\sigma^s, \tau_\sigma^e]$, one can consider the probability of detecting no electrons in the spatial interval $[v_F\tau_\sigma^s, v_F\tau_\sigma^e]$ (Fig. 1). We define the single-particle projection operator

$$\widehat{\mathcal{Q}}_\sigma = \int_{v_F\tau_\sigma^s}^{v_F\tau_\sigma^e} \hat{b}_\sigma^\dagger(x)\hat{b}_\sigma(x) dx, \tag{14}$$

which measures the probability of finding a spin-σ electron in the spatial interval $x_\sigma \in [v_F\tau_\sigma^s, v_F\tau_\sigma^e]$ in the right lead, where $\hat{b}_\sigma^{(\dagger)}(x)$ annihilate (create) spin-σ electrons at position x (Fig. 1). The generalized ITP [69], $\Pi(\tau_\uparrow^s, \tau_\uparrow^e; \tau_\downarrow^s, \tau_\downarrow^e)$, is the joint probability that no spin-σ electrons are detected during the time intervals $[\tau_\sigma^s, \tau_\sigma^e]$. It can be expressed as the expectation value of the normal-ordered exponent of $-\sum_\sigma \widehat{\mathcal{Q}}_\sigma$,

$$\Pi(\tau_\uparrow^s, \tau_\uparrow^e; \tau_\downarrow^s, \tau_\downarrow^e) = \langle : e^{-\sum_\sigma \widehat{\mathcal{Q}}_\sigma} : \rangle, \tag{15}$$

with $: \cdot :$ denoting the normal ordering of operators [69]. One may evaluate the average and obtain the ITP in a determinant form [69],

$$\Pi(\tau_\uparrow^s, \tau_\uparrow^e; \tau_\downarrow^s, \tau_\downarrow^e) = \det(\mathbf{I} - \mathbf{Q}_{(\tau_\sigma^s, \tau_\sigma^e)}). \tag{16}$$

The matrix $\mathbf{Q}$ is a 2×2 block matrix in the spin space with the form [69]

$$\mathbf{Q}_{(\tau_\sigma^s, \tau_\sigma^e)}(E, E') = \mathbf{t}^\dagger(E)\mathbf{K}(E - E')\mathbf{t}(E'). \tag{17}$$

Here, the kernel matrix is diagonal in spin space and reads as [69]

$$\mathbf{K}_{\sigma\sigma}(E) = \frac{\kappa}{\pi} e^{-iE(\tau_\sigma^s + \tau_\sigma^e)/2} \frac{\sin\left[E\left(\tau_\sigma^s - \tau_\sigma^e\right)/2\right]}{E}. \tag{18}$$

In calculating the determinant, given by Eq. (16), we have divided the transport window into N energy elements, each with size $\kappa = eV/N$. A large N should be taken to ensure the numerical convergence.

The two-channel ITP $\Pi(\tau^s, \tau^e)$, the probability of detecting no electron regardless of the spin degree in any of the outgoing channels during a time interval $[\tau^s, \tau^e]$, can be obtained from

the generalized ITP by setting $\tau^e_\uparrow = \tau^e_\downarrow = \tau^e$, $\tau^s_\uparrow = \tau^s_\downarrow = \tau^s$. The ITP for a single spin-σ channel can be obtained from the generalized ITP as $\Pi_\sigma(\tau^s_\sigma,\tau^e_\sigma) \equiv \Pi(\tau^s_\sigma,\tau^e_\sigma;\tau^s_{\bar\sigma} = \tau^e_{\bar\sigma})$. Here and below, we use notation $\bar\sigma$ to denote the spin index which is different from σ, with $\bar\sigma = \downarrow$ for $\sigma = \uparrow$, and $\bar\sigma = \uparrow$ for $\sigma = \downarrow$.

The joint probability density of detecting two successive electrons both at τ^s and τ^e is equal to the WTDs multiplied by the probability density of a detection event at τ^s. For the unidirectional quantum transport considered in this work, the probability density of a detection at τ^s is simply the electronic current $I(\tau^s)$ without distinguishing spin or spin current $I_{R\sigma}(\tau^s)$ for a specific spin channel. The joint probability density can also be obtained by differentiating the ITPs with respect to both the starting time τ^s and the ending time τ^e. Then we can get the equations for two-channel WTD, spin-resolved single-channel WTD, and cross-channel WTD, respectively, as [69]

$$I(\tau^s)\mathcal{W}(\tau^s,\tau^e) = -\partial_{\tau^s}\partial_{\tau^e}\Pi(\tau^s,\tau^e), \tag{19}$$

$$I_{R\sigma}(\tau^s)\mathcal{W}_{\sigma\sigma}(\tau^s,\tau^e) = -\partial_{\tau^s}\partial_{\tau^e}\Pi_\sigma(\tau^s,\tau^e), \tag{20}$$

$$I_{R\sigma}(\tau^s)\mathcal{W}_{\sigma\bar\sigma}(\tau^s,\tau^e) = -\partial_{\tau^s}\partial_{\tau^e}\Pi(\tau^s_\sigma,\tau^e;\tau^s,\tau^e)\big|_{\tau^s_\sigma=\tau^s}. \tag{21}$$

For the dc transport at zero temperature, the electronic current is the inverse mean waiting time [62,69], so that we have $I(\tau^s) = 1/\langle\tau\rangle$ and $I_{R\sigma}(\tau^s) = 1/\langle\tau_\sigma\rangle$, where $\langle\tau\rangle$ is the average two-channel waiting time and $\langle\tau_\sigma\rangle$ is the average spin-resolved single-channel waiting time. Since the dc quantum transport possesses the time translational symmetry, WTDs and ITPs only depend on the time difference $\tau = \tau^e - \tau^s$, and one can write the above expressions of WTD as [69]

$$\mathcal{W}(\tau) = \langle\tau\rangle\frac{\partial^2\Pi(\tau)}{\partial\tau^2}, \tag{22}$$

$$\mathcal{W}_{\sigma\sigma}(\tau) = \langle\tau_\sigma\rangle\frac{\partial^2\Pi_\sigma(\tau)}{\partial\tau^2}, \tag{23}$$

$$\mathcal{W}_{\sigma\bar\sigma}(\tau) = \langle\tau_\sigma\rangle\frac{\partial^2\Pi(\tau^s_\sigma,\tau^e;\tau^s,\tau^e)}{\partial\tau^s_\sigma\partial\tau^e}\bigg|_{\tau^s_\sigma=\tau^s;\ \tau^e-\tau^s=\tau}. \tag{24}$$

The formalism presented is used to calculate WTDs for the noninteracting systems at zero temperature and assumes a linear dispersion relation with respect to the momentum in the electronic reservoir. It assumes neither Markovian approximation nor any renewal properties.

The first-passage time distribution (FPTD) $\mathcal{F}_\sigma(\tau^s_\sigma,\tau')$ is the probability density for the event to occur at a time τ', in spite of the observation result of the previous time τ^s_σ [52,69,76]. One can relate the FPTD of the spin-σ channel with the corresponding ITP through the relation

$$1 - \int_{\tau^s_\sigma}^{\tau^e_\sigma}\mathcal{F}_\sigma(\tau^s_\sigma,\tau')d\tau' = \Pi_\sigma(\tau^s_\sigma,\tau^e_\sigma;\tau^s_{\bar\sigma} = \tau^e_{\bar\sigma}). \tag{25}$$

The time integral in the above equation represents the probability to detect spin-σ electrons during the time interval $[\tau^s_\sigma,\tau^e_\sigma]$. For dc quantum transport, the FPTD is expressed as [76]

$$\mathcal{F}_\sigma(\tau) = -\partial_\tau\Pi_\sigma(\tau). \tag{26}$$

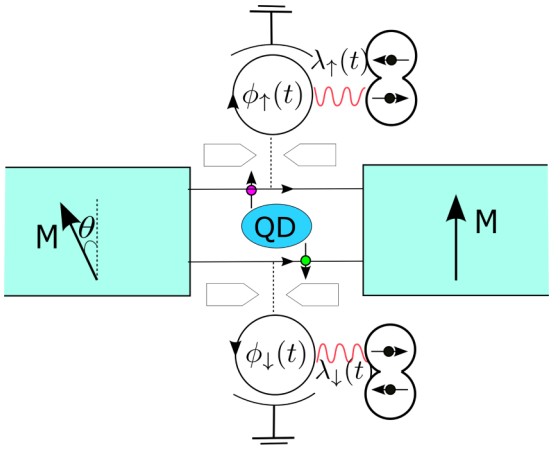

FIG. 2. Schematic plot of spin-resolved waiting-time clock. A quantum spin Hall QD is embedded between two ferromagnetic electrodes. Spin-σ (spin-up in the plot) electrons can tunnel into the capacitor through a quantum point contact and then interact with a two-level system. Spin-σ electron waiting times can be obtained from monitoring the two-level system by changing interaction strength $\lambda_\sigma(t)$.

If the outgoing spin-up and -down channels are uncorrelated, the detection result of a later time in one channel does not depend on the earlier detection in the other channel, so that the cross-channel WTD for uncorrelated spin channels is equal to the FPTD [69],

$$\mathcal{W}^{uc}_{\sigma\bar\sigma}(\tau) = \mathcal{F}_{\bar\sigma}(\tau). \tag{27}$$

In order to measure WTD above the Fermi sea experimentally, a quantum formalism of a detector, which is called waiting-time clock, has been proposed [67]. The waiting-time clock consists of a mesoscopic capacitor being coupled to a quantum two-level system. The electrons from the system transmit to a chiral edge state in the quantum Hall regime and then tunnel into the capacitor through a quantum point contact. The quantum point contact only transmits the electrons above the Fermi sea. Electrons inside the capacitor interact with a two-level system of which we monitor the coherent precession, and then leave the capacitor. The coupling strength $\lambda(t)$ between the two-level system and the capacitor is tunable and time dependent. The moment-generating function could be obtained from reading the off-diagonal element of the density matrix of the two-level system for different coupling strengths λ. Then one can get the ITP from the moment-generating function, and hence WTD. The chiral edge state is needed here so that the electron can tunnel into the capacitor through a quantum point contact. For the system presented in our work, we consider the QD to be a quantum spin Hall (QSH) quantum dot [70–72] (see Fig. 2) in order to have edge states in the QD spin valve. When the the Fermi wavelengths are longer than the distance between two ferromagnetic electrodes, the spin-dependent scattering can open a gap to form a dot in a system such as the double HgTe/CdTe quantum well [77]. One can also use QSH edges in contact to the QD [78,79] to form chiral edge states in the central scattering region. When the Fermi energy of QD is inside the energy gap, electrons only tunnel through the unidirectional spin-locked edge state, and

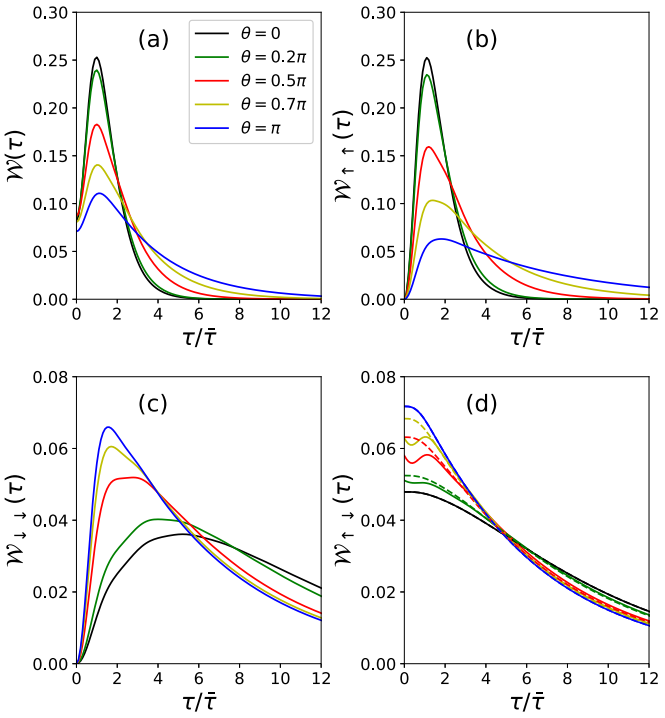

FIG. 3. (a) Two-channel WTD $\mathcal{W}(\tau)$, (b) spin-up WTD $\mathcal{W}_{\uparrow\uparrow}(\tau)$, (c) spin-down WTD $\mathcal{W}_{\downarrow\downarrow}(\tau)$, and (d) cross-channel WTD $\mathcal{W}_{\uparrow\downarrow}(\tau)$ are plotted by varying noncollinear angle θ with spin polarization $p = 0.8$. The corresponding FPTD for spin-down $\mathcal{F}_{\downarrow}(\tau)$ is plotted with a dashed line in (d). The waiting time is in units of time, $\bar{\tau} = h/(eV)$.

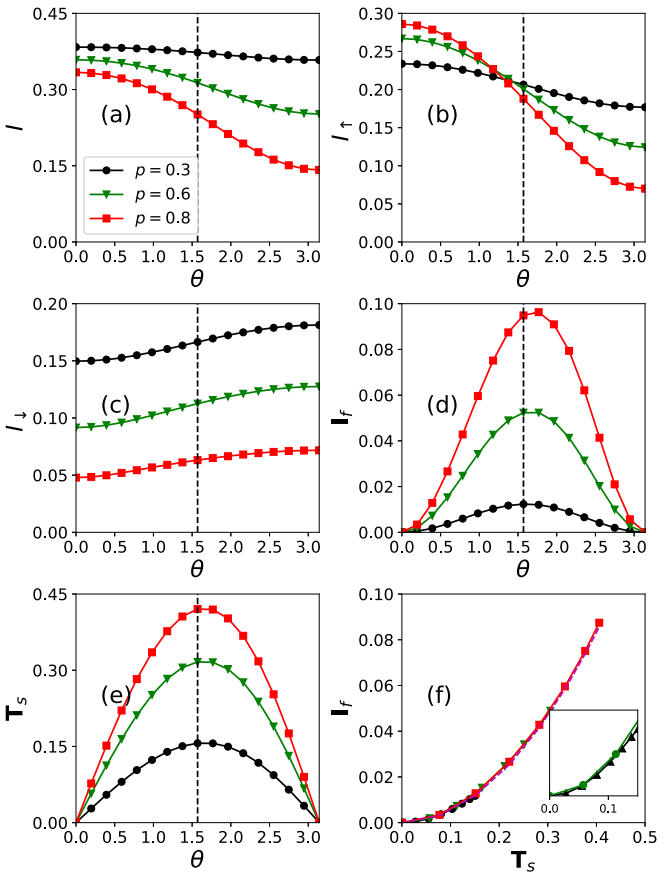

FIG. 4. (a) Charge current, (b) spin-up current $I_{R\uparrow}$, (c) spin-down current $I_{R\downarrow}$, (d) influence degree, and (e) $\mathbf{T}_s$ vs noncollinear angle θ with different spin polarization p. (f) Influence degree vs $\mathbf{T}_s$ with the quadratic fitting $\mathbf{I}_f = 0.51(\mathbf{T}_s)^2$ shown as dashed lines.

one can use one edge to transmit spin-up electrons and the other edge to transmit spin-down electrons. Then the spin-σ WTD can be measured by measuring the two-level system with which the spin-σ electrons interact. The waiting-time clock involving cross-channel detection is also worth future investigation.

III. NUMERICAL RESULTS AND DISCUSSION

In this section, the numerical outcome on the WTDs of the QD spin valve by varying noncollinear angle θ and spin polarization p is reported. We choose the lead coupling strength Γ as the energy unit. Voltage bias $eV = 3\Gamma$ is applied on the left lead. In the following calculation, the QD levels are set within the transport window with $\epsilon_{\uparrow} = 2.0\Gamma$ and $\epsilon_{\downarrow} = 1.5\Gamma$ for resonant transport, except for Fig. 5, wherein $\epsilon_{\uparrow} = \epsilon_{\downarrow} = 5.0\Gamma$ for off-resonant transport. The waiting time τ is in units of the fundamental time scale $\bar{\tau} = h/(eV)$, which is the average time separation of the emitted electrons from the left lead.

In Fig. 3, we plot the two-channel WTD $\mathcal{W}(\tau)$ [Fig. 3(a)], spin-up WTD $\mathcal{W}_{\uparrow\uparrow}(\tau)$ [Fig. 3(b)], spin-down WTD $\mathcal{W}_{\downarrow\downarrow}(\tau)$ [Fig. 3(c)], and cross-channel WTD $\mathcal{W}_{\uparrow\downarrow}(\tau)$ [Fig. 3(d)] by varying noncollinear angle θ with spin polarization $p = 0.8$. The FPTDs for spin-down electrons $\mathcal{F}_{\downarrow}(\tau)$ are plotted with dashed lines in Fig. 3(d). $\theta = 0$ and $\theta = \pi$ corresponds to parallel and antiparallel configuration, respectively. Differently from the single-channel case where the Pauli exclusion principle does not allow two electrons to occupy the same state, two electrons from different spin channels can be detected at the same time, so that two-channel WTD is nonzero at $\tau = 0$. Two-channel WTD takes its maximal value at $\tau = \bar{\tau}$, and this is the same as that of a spinless system [62]. With a positive polarization, spin-up and -down states are majority and minority states in the left lead, respectively. The spin-up current in the right lead has contributions from both the spin-up and spin-down electrons in the left lead. Increasing θ from 0 to π, the contribution to $I_{R\uparrow}$ from the spin-up (majority state) electrons in the left lead decreases, and the contribution from the spin-down (minority state) electrons increases. The combined effect leads to a decreasing spin-up current $I_{R\uparrow}$ in the right lead with increasing θ. Due to a similar argument, one can explain that spin-down current $I_{R\downarrow}$ increases with increasing θ. The particle current, as the sum of spin-up and spin-down current, decreases with increasing θ. These current behaviors with respect to noncollinear angle θ are shown in Figs. 4(a)–4(c). As can be observed from Figs. 3(a)–3(c), two-channel WTD $\mathcal{W}(\tau)$ and spin-up WTD $\mathcal{W}_{\uparrow\uparrow}(\tau)$ decrease with increasing θ at initial short times which are around before $\tau = 5\bar{\tau}$, and spin-down WTD $\mathcal{W}_{\downarrow\downarrow}(\tau)$ and cross-channel WTD $\mathcal{W}_{\uparrow\downarrow}(\tau)$ increase with increasing θ at initial short times. Comparing the behaviors between currents and WTDs, one can observe that both particle current and two-channel WTD at initial short times decrease with increasing θ, and $I_{R\sigma}$ and $\mathcal{W}_{\sigma'\sigma}(\tau)$ at initial short times share the same monotonicity. The maximum point of $\mathcal{W}_{\downarrow\downarrow}(\tau)$ shifts towards shorter times with

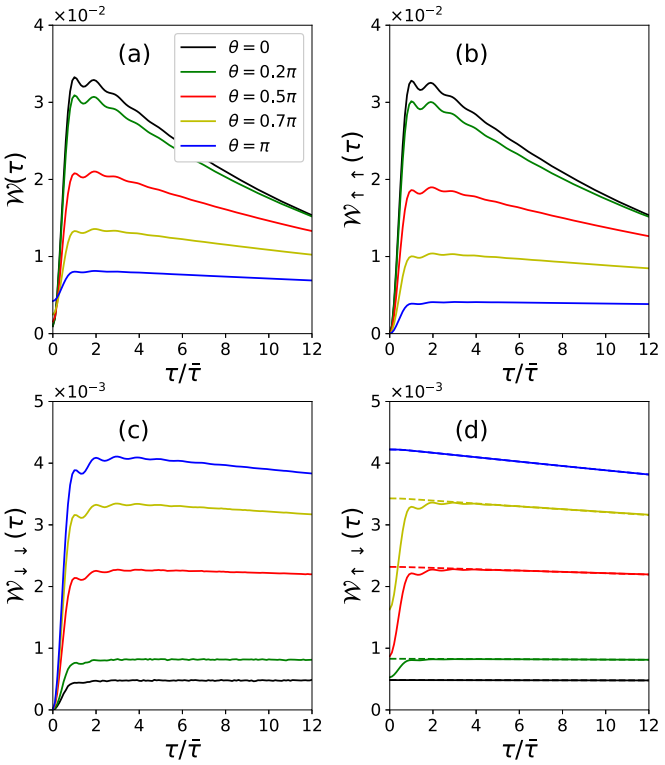

FIG. 5. WTDs for off-resonant transport corresponding to Fig. 3 with $\epsilon_\uparrow = \epsilon_\downarrow = 5\Gamma$.

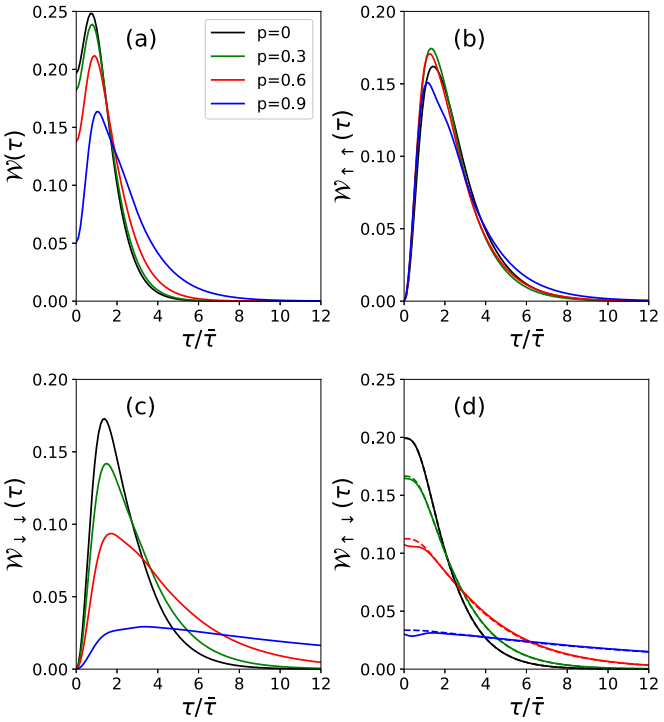

FIG. 6. (a) Two-channel WTD $\mathcal{W}(\tau)$, (b) spin-up WTD $\mathcal{W}_{\uparrow\uparrow}(\tau)$, (c) spin-down WTD $\mathcal{W}_{\downarrow\downarrow}(\tau)$, and (d) cross-channel WTD $\mathcal{W}_{\uparrow\downarrow}(\tau)$ are plotted by varying spin polarization p with $\theta = \pi/2$. The corresponding FPTD for spin-down $\mathcal{F}_\downarrow(\tau)$ is plotted with a dashed line in (d).

increasing angle θ from 0 to π and this indicates the increasing of the tunnel magnitude to the spin-down state in the right lead as well.

In Fig. 3(d), FPTDs for spin-down $\mathcal{F}_\downarrow(\tau)$ are plotted using dashed lines in comparison with the corresponding cross-channel WTD $\mathcal{W}_{\uparrow\downarrow}(\tau)$. We can observe that FPTD and WTD coincide with each other for the collinear configurations with $\theta = 0$ and $\theta = \pi$ since the two spin channels are uncorrelated. Once the spin valve is in the noncollinear setup, cross-channel WTD deviates from its corresponding FPTD and this indicates the occurrence of spin torque transfer during transport. Cross-channel WTDs are less than FPTDs at initially short times and this indicates the suppression of subsequent detection due to the correlation between two spin channels and Pauli exclusion principle. One can observe that FPTD is a monotonically decreasing function with respect to the time, while cross-channel WTD may not have this property.

In order to better demonstrate the influence of the first detection on the subsequent detection result from the perspective of cross-channel WTD, the influence degree quantity is defined as the cumulative absolute difference between cross-channel WTDs and FPTDs with the expression

$$\mathbf{I}_f = \sum_\sigma \int_0^\infty |\mathcal{W}_{\bar{\sigma}\sigma}(\tau) - \mathcal{F}_\sigma(\tau)| d\tau. \tag{28}$$

We plot the influence degree versus θ by varying spin polarization p in Fig. 4(d), and the influence degree versus spin polarization p by varying θ in Fig. 7(d). One can see that the influence degree vanishes for linear configurations with $\theta = 0$ and $\theta = \pi$, and reaches its maximum near angle $\theta = \pi/2$ in which STT also achieves its maximal value [14–16].

If one tunes the QD levels far away from the resonant condition, it can mimic the behaviors of MTJ with an insulating scattering region. WTDs for off-resonant transport corresponding to Fig. 3 with $\epsilon_\uparrow = \epsilon_\downarrow = 5\Gamma$ are plotted in Fig. 5. One can see that there are small oscillations with period $\bar{\tau}$ for all the WTDs shown in Fig. 5 at initial short times due to the small transmission amplitude in the off-resonant condition [62]. The behaviors of WTDs at short times are with respect to noncollinear angle θ.

In Fig. 6, we plot the WTDs by varying spin polarization p with noncollinear angle $\theta = \pi/2$ for the resonant transport. The corresponding FPTDs $\mathcal{F}_\downarrow(\tau)$ are plotted with dashed lines in Fig. 6(d). Increasing the polarization reduces both the particle current and spin-down electronic current so that two-channel WTD $\mathcal{W}(\tau)$, spin-down WTD $\mathcal{W}_{\downarrow\downarrow}(\tau)$, and cross-channel WTD $\mathcal{W}_{\uparrow\downarrow}(\tau)$ decrease at initial short times with increasing p. As indicated in Fig. 7(b), the spin-up current is not monotonic with respect to polarization p at $\theta = 0.5\pi$, as is the short-time behavior of spin-up WTD $\mathcal{W}_{\uparrow\uparrow}(\tau)$. The short-time behavior of $\mathcal{W}_{\sigma'\sigma}(\tau)$ is the same as spin-σ current $I_{R\sigma}$ by changing polarization p and can be seen by comparing Figs. 6 and 7. With $p \to 1$, both leads become a half-metallic ferromagnet with only spin-up channel, $\mathcal{W}(\tau = 0) \to 0$, due to the Pauli exclusion principle. When both leads are normal metal, i.e., $p = 0$, spin-up and -down channels are uncorrelated and there is no spin-flip process through the junction, and, as can be seen from Fig. 6(d), cross-channel WTD $\mathcal{W}_{\uparrow\downarrow}(\tau)$ coin-

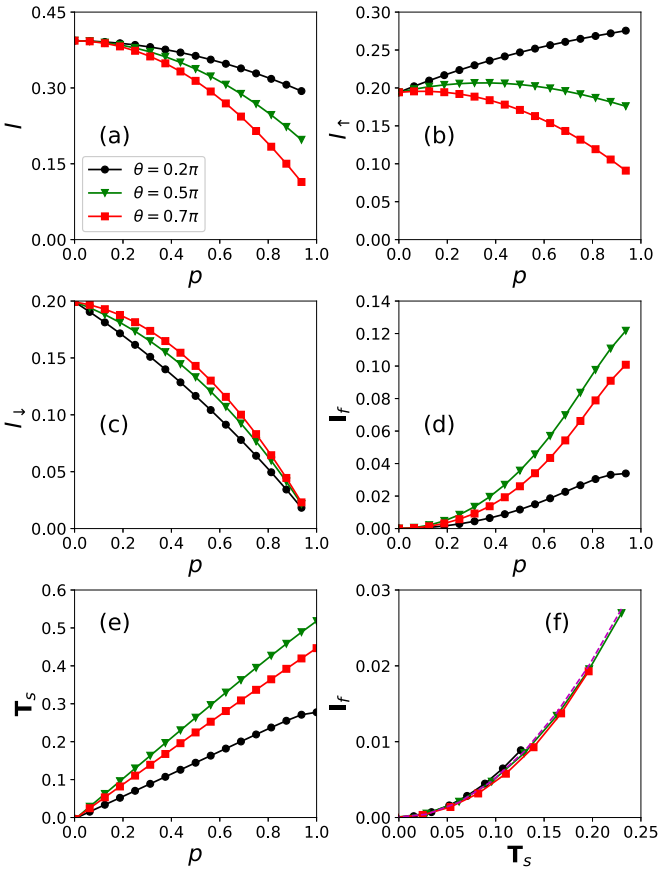

FIG. 7. (a) Charge current, (b) spin-up current $I_{R\uparrow}$, (c) spin-down current $I_{R\downarrow}$, (d) influence degree, and (e) $\mathbf{T_s}$ vs spin polarization p with different noncollinear angles θ. (f) Influence degree vs $\mathbf{T_s}$ with the quadratic fitting $\mathbf{I}_f = 0.51(\mathbf{T}_s)^2$ shown as dashed lines.

cides with FPTD $\mathcal{F}_\downarrow(\tau)$. One can observe from Fig. 7(d) that the influence degree is zero for $p = 0$, and this is independent of angle θ. Influence degree is an increment function with respect to the spin polarization regardless of noncollinear angle, as can be seen from Figs. 4(d) and 7(d). Cross-channel WTDs are less than FPTDs at initially short times by varying polarization, and this is also due to spin-channel correlation.

We plot the corresponding spin-transfer torque (STT) versus noncollinear angle θ with different spin polarization p in Fig. 4(e), and versus spin polarization with different noncollinear angle θ in Fig. 7(e). In order to show that spin-resolved waiting times can directly reflect STT, we show a one-to-one correspondence between STT and the influence degree quantity ($\mathbf{I}_f$) in Figs. 4(f) and 7(f). The noncollinear angle θ takes the value in the range $[0,\pi/2]$ in Fig. 4(f). We can see that by varying noncollinear angle θ and polarization p, there is always a specific value of influence degree ($\mathbf{I}_f$) corresponding to a given STT. We also find that they can be very well fitted by a quadratic relation $\mathbf{I}_f = 0.51(\mathrm{STT})^2$, plotted as dashed lines in Figs. 4(f) and 7(f). Finally, from Figs. 4(f) and 7(f), we see that $\mathbf{I}_f$ versus STT for different noncollinear angles as well as different polarizations collapse into a single curve showing universal behaviors. This demonstrates that the behaviors of spin-resolved waiting times and STT are closely related.

IV. CONCLUSION

In this work, we employ the scattering matrix approach to study the WTDs in a QD spin valve at zero temperature. The WTDs and FPTDs are calculated by taking derivatives with respect to the ITP which is a determinant involving both the spin and energy space. The behaviors of two-channel WTD, spin-up WTD, spin-down WTD, and cross-channel WTD are numerically shown with respect to noncollinear angle and spin polarization. Two-channel WTD takes its maximal value at $\tau = \bar{\tau}$ and is nonzero at $\tau = 0$, which is due to the possibility of detecting two electrons from different spin channels at the same time. The short-time behaviors of two-channel WTD and $\mathcal{W}_{\sigma'\sigma}(\tau)$ are the same as particle current and spin-σ current $I_{R\sigma}$, respectively. We observe that FPTD and WTD coincide with each other for the collinear configurations, wherein the spin channels are uncorrelated. When the spin valve is in the noncollinear setup, the deviation of cross-channel WTD from its corresponding FPTD indicates the occurrence of spin torque transfer across the junction. Cross-channel WTD is less than the corresponding FPTD at initially short times and this indicates the suppression of subsequent detection due to the correlation between the two spin channels. We introduce the "influence degree" quantity to quantitatively characterize the correlation strength of the spin channels. We find that the influence degree vanishes for linear configurations and reaches its maximum near angle $\theta = \pi/2$ in which STT also achieves its maximal value. Since spin-correlation strength increases with increasing spin polarization, influence degree is an increment function with respect to the spin polarization. We have shown that the influence degree quantity is nonvanishing for the systems with a spin-flip process. We further observe that influence degree versus spin-transfer torque for different noncollinear angles as well as different polarizations collapses into to a single curve showing universal behaviors. This work enables us to see that cross-channel WTD can be a pathway to characterize properties in spintronics and motivates us to study waiting-time distribution in other spintronics systems in the future.

ACKNOWLEDGMENTS

F.X. is financially supported by the National Natural Science Foundation of China (Grant No. 11504240) and Shenzhen Key Lab Fund (Grant No. 20170228105421966). G.T. and J.W. are financially supported by NSF-China (Grant No. 11374246), the GRF (Grant No. 17311116), and the UGC (Contract No. AoE/P-04/08) of the Government of HKSAR.

[1] S. A. Wolf and D. Treger, IEEE Trans. Magn. **36**, 2748 (2000).
[2] S. A. Wolf, D. D. Awschalom, R. A. Buhrman, J. M. Daughton, S. von Molnaár, M. L. Roukes, A. Y. Chtchelkanova, and D. M. Treger, Science **294**, 1488 (2001).
[3] I. Žutić, J. Fabian, and S. Das Sarma, Rev. Mod. Phys. **76**, 323 (2004).
[4] J. König and J. Martinek, Phys. Rev. Lett. **90**, 166602 (2003).

[5] M. Braun, J. König, and J. Martinek, Phys. Rev. B **70**, 195345 (2004).
[6] K. Gong, L. Zhang, L. Liu, Y. Zhu, G. Yu, P. Grutter, and H. Guo, J. Appl. Phys. **118**, 093902 (2016).
[7] M. Julliere, Phys. Lett. A **54**, 225 (1975).
[8] J. C. Slonczewski, Phys. Rev. B **39**, 6995 (1989).
[9] S. S. P. Parkin, C. Kaiser, A. Panchula, P. M. Rice, B. Hughes, M. Samant, and S.-H. Yang, Nat. Mater. **3**, 862 (2004).
[10] J. C. Sankey, Y.-T. Cui, J. Z. Sun, J. C. Slonczewski, R. A. Buhrman, and D. C. Ralph, Nat. Phys. **4**, 67 (2008).
[11] J. Mathon and A. Umerski, Phys. Rev. B **63**, 220403(R) (2001).
[12] J. C. Slonczewski, J. Magn. Magn. Mater. **159**, L1 (1996).
[13] L. Berger, Phys. Rev. B **54**, 9353 (1996).
[14] I. Theodonis, N. Kioussis, A. Kalitsov, M. Chshiev, and W. H. Butler, Phys. Rev. Lett. **97**, 237205 (2006).
[15] I. Theodonis, A. Kalitsov, and N. Kioussis, Phys. Rev. B **76**, 224406 (2007).
[16] A. Kalitsov, M. Chshiev, I. Theodonis, N. Kioussis, and W. H. Butler, Phys. Rev. B **79**, 174416 (2009).
[17] X. Jia, K. Xia, and G. E. W. Bauer, Phys. Rev. Lett. **107**, 176603 (2011).
[18] H. Kubota, A. Fukushima, K. Yakushiji, T. Nagahama, S. Yuasa, K. Ando, H. Maehara, Y. Nagamine, K. Tsunekawa, D. D. Djayaprawira, N. Watanabe, and Y. Suzuki, Nat. Phys. **4**, 37 (2008).
[19] D. C. Ralph and M. D. Stiles, J. Magn. Magn. Mater. **320**, 1190 (2008).
[20] Y. Dubi and M. Di Ventra, Phys. Rev. B **79**, 081302(R) (2009).
[21] R. Świrkowicz, M. Wierzbicki, and J. Barnaś, Phys. Rev. B **80**, 195409 (2009).
[22] G. E. W. Bauer, E. Saitoh, and B. J. van Wees, Nat. Mater. **11**, 391 (2012).
[23] A. B. Cahaya, O. A. Tretiakov, and G. E. W. Bauer, IEEE Trans. Magn. **51**, 0800414 (2015).
[24] G. Tang, J. Thingna, and J. Wang, arXiv:1802.06549.
[25] J. Fransson, Phys. Rev. B **72**, 045415 (2005).
[26] J. N. Pedersen, J. Q. Thomassen, and K. Flensberg, Phys. Rev. B **72**, 045341 (2005).
[27] I. Weymann and J. Barnaś, Phys. Rev. B **75**, 155308 (2007).
[28] J. Splettstoesser, M. Governale, and J. Konig, Phys. Rev. B **77**, 195320 (2008).
[29] P. Virtanen and T. T. Heikkilä, Phys. Rev. Lett. **118**, 237701 (2017).
[30] Y. Yu, H. Zhan, L. Wan, B. Wang, Y. Wei, Q. Sun, and J. Wang, Nanotechnology **24**, 155202 (2013).
[31] Ya. Blanter and M. Büttiker, Phys. Rep. **336**, 1 (2000).
[32] L. S. Levitov and G. B. Lesovik, Pis'ma Zh. Eksp. Teor. Fiz. **58**, 225 (1993) [Sov. Phys. JETP Lett. **58**, 230 (1993)].
[33] L. S. Levitov, H.-W. Lee, and G. B. Lesovik, J. Math. Phys. **37**, 4845 (1996).
[34] C. Flindt, T. Novotný, A. Braggio, M. Sassetti, and A. P. Jauho, Phys. Rev. Lett. **100**, 150601 (2008).
[35] F. Hassler, M. V. Suslov, G. M. Graf, M. V. Lebedev, G. B. Lesovik, and G. Blatter, Phys. Rev. B **78**, 165330 (2008).
[36] C. Flindt, T. Novotný, A. Braggio, and A. P. Jauho, Phys. Rev. B **82**, 155407 (2010).
[37] F. Domínguez, G. Platero, and S. Kohler, Chem. Phys. **375**, 284 (2010).
[38] V. F. Maisi, D. Kambly, C. Flindt, and J. P. Pekola, Phys. Rev. Lett. **112**, 036801 (2014).
[39] G.-M. Tang and J. Wang, Phys. Rev. B **90**, 195422 (2014).
[40] B. K. Agarwalla, H. Li, B. Li, and J.-S. Wang, Phys. Rev. E **89**, 052101 (2014).
[41] R. S. Souto, A. Martín-Rodero, and A. L. Yeyati, Phys. Rev. Lett. **117**, 267701 (2016).
[42] G. Tang, Z. Yu, and J. Wang, New J. Phys. **19**, 083007 (2017).
[43] G. Tang, Y. Xing, and J. Wang, Phys. Rev. B **96**, 075417 (2017).
[44] G. Tang, X. Chen, J. Ren, and J. Wang, Phys. Rev. B **97**, 081407(R) (2018).
[45] R. S. Souto, A. Martín-Rodero, and A. L. Yeyati, Phys. Rev. B **96**, 165444 (2017).
[46] M. Ridley, V. N. Singh, E. Gull, and G. Cohen, Phys. Rev. B **97**, 115109 (2018).
[47] S. Lindebaum, D. Urban, and J. König, Phys. Rev. B **79**, 245303 (2009).
[48] Y. Utsumi and T. Taniguchi, Phys. Rev. Lett. **114**, 186601 (2015).
[49] M. A. Kastner, Rev. Mod. Phys. **64**, 849 (1992).
[50] D. L. Klein, R. Roth, A. K. L. Lim, A. P. Alivisatos, and P. L. McEuen, Nature (London) **389**, 699 (1997).
[51] J. Martin, N. Akerman, G. Ulbricht, T. Lohmann, J. H. Smet, K. von Klitzing, and A. Yacoby, Nat. Phys. **4**, 144 (2008).
[52] N. G. van Kampen, *Stochastic Processes in Physics and Chemistry* (Elsevier, Amsterdam, 2007).
[53] T. Brandes, Ann. Phys. **17**, 477 (2008).
[54] S. Welack, S. Mukamel, and Y. Yan, Europhys. Lett. **85**, 57008 (2009).
[55] M. Albert, C. Flindt, and M. Büttiker, Phys. Rev. Lett. **107**, 086805 (2011).
[56] L. Rajabi, C. Poltl, and M. Governale, Phys. Rev. Lett. **111**, 067002 (2013).
[57] B. Sothmann, Phys. Rev. B **90**, 155315 (2014).
[58] D. S. Kosov, J. Chem. Phys. **146**, 074102 (2017).
[59] E. Potanina and C. Flindt, Phys. Rev. B **96**, 045420 (2017).
[60] N. Walldorf, C. Padurariu, A.-P. Jauho, and C. Flindt, Phys. Rev. Lett. **120**, 087701 (2018).
[61] K. H. Thomas and C. Flindt, Phys. Rev. B **87**, 121405 (2013).
[62] M. Albert, G. Haack, C. Flindt, and M. Büttiker, Phys. Rev. Lett. **108**, 186806 (2012).
[63] K. H. Thomas and C. Flindt, Phys. Rev. B **89**, 245420 (2014).
[64] D. Dasenbrook, C. Flindt, and M. Buttiker, Phys. Rev. Lett. **112**, 146801 (2014).
[65] M. Albert and P. Devillard, Phys. Rev. B **90**, 035431 (2014).
[66] P. P. Hofer, D. Dasenbrook, and C. Flindt, Physica E (Amsterdam) **82**, 3 (2016).
[67] D. Dasenbrook and C. Flindt, Phys. Rev. B **93**, 245409 (2016).
[68] G. Haack, M. Albert, and C. Flindt, Phys. Rev. B **90**, 205429 (2014).
[69] D. Dasenbrook, P. P. Hofer, and C. Flindt, Phys. Rev. B **91**, 195420 (2015).
[70] C. Timm, Phys. Rev. B **86**, 155456 (2012).
[71] G. Dolcetto, N. Traverso Ziani, M. Biggio, F. Cavaliere, and M. Sassetti, Phys. Rev. B **87**, 235423 (2013).
[72] N. Traverso Ziani, C. Fleckenstein, G. Dolcetto, and B. Trauzettel, Phys. Rev. B **95**, 205418 (2017).

[73] S. Datta, *Electronic Transport in Mesoscopic Systems* (Cambridge University Press, Cambridge, 1997).
[74] J. Wang and H. Guo, Phys. Rev. B **79**, 045119 (2009).
[75] A. Nock, S. Kumar, H.-J. Sommers, and T. Guhr, Ann. Phys. **342**, 103 (2014).
[76] G.-M. Tang, F. Xu, and J. Wang, Phys. Rev. B **89**, 205310 (2014).
[77] P. Michetti, J. C. Budich, E. G. Novik, and P. Recher, Phys. Rev. B **85**, 125309 (2012).
[78] B. Rizzo, A. Camjayi, and L. Arrachea, Phys. Rev. B **94**, 125425 (2016).
[79] Y. Xing, Z. L. Yang, Q. F. Sun, and J. Wang, Phys Rev. B **90**, 075435 (2014).